Pediatr Radiol (2016) 46:1282–1290
DOI 10.1007/s00247-016-3611-1

ORIGINAL ARTICLE

Imaging features of kaposiform lymphangiomatosis

Pradeep Goyal[1,2] · **Ahmad I. Alomari**[1,2] · **Harry P. Kozakewich**[1,3] · **Cameron C. Trenor III**[1,4] · **Antonio R. Perez-Atayde**[1,3] · **Steven J. Fishman**[1,5] · **Arin K. Greene**[1,6] · **Raja Shaikh**[1,2] · **Gulraiz Chaudry**[1,2]

Received: 11 October 2015 / Revised: 24 January 2016 / Accepted: 14 March 2016 / Published online: 6 April 2016

Abstract
Background Kaposiform lymphangiomatosis is a rare, aggressive lymphatic disorder. The imaging and presenting features of kaposiform lymphangiomatosis can overlap with those of central conducting lymphatic anomaly and generalized lymphatic anomaly.
Objective To analyze the imaging findings of kaposiform lymphangiomatosis disorder and highlight features most suggestive of this diagnosis.
Materials and methods We retrospectively identified and characterized 20 children and young adults with histopathological diagnosis of kaposiform lymphangiomatosis and radiologic imaging referred to the vascular anomalies center between 1995 and 2015.
Results The median age at onset was 6.5 years (range 3 months to 27 years). The most common presenting features were respiratory compromise (dyspnea, cough, chest pain; 55.5%), swelling/mass (25%), bleeding (15%) and fracture (5%). The thoracic cavity was involved in all patients; all patients had mediastinal involvement followed by lung parenchymal disease (90%) and pleural (85%) and pericardial (50%) effusions. The most common extra-thoracic sites of disease were the retroperitoneum (80%), bone (60%), abdominal viscera (55%) and muscles (45%). There was characteristic enhancing and infiltrative soft-tissue thickening in the mediastinum and retroperitoneum extending along the lymphatic distribution.
Conclusion Kaposiform lymphangiomatosis has overlapping imaging features with central conducting lymphatic anomaly and generalized lymphatic anomaly. Presence of mediastinal or retroperitoneal enhancing and infiltrative soft-tissue disease along the lymphatic distribution, hemorrhagic effusions and moderate thrombocytopenia (50–100,000/μl) should favor diagnosis of kaposiform lymphangiomatosis.

Keywords Children · Computed tomography · Kaposiform lymphangiomatosis · Lymphatic malformation · Magnetic resonance imaging · Radiography · Ultrasound

✉ Gulraiz Chaudry
gulraiz.chaudry@childrens.harvard.edu

1 Vascular Anomalies Center, Boston Children's Hospital and Harvard Medical School, Boston, MA, USA

2 Division of Vascular and Interventional Radiology, Boston Children's Hospital and Harvard Medical School, 300 Longwood Ave., Boston, MA 02115, USA

3 Department of Pathology, Boston Children's Hospital and Harvard Medical School, Boston, MA, USA

4 Division of Hematology/Oncology, Boston Children's Hospital and Harvard Medical School, Boston, MA, USA

5 Department of Surgery, Boston Children's Hospital and Harvard Medical School, Boston, MA, USA

6 Department of Plastic and Oral Surgery, Boston Children's Hospital and Harvard Medical School, Boston, MA, USA

Introduction

Kaposiform lymphangiomatosis is a rare, complex lymphatic disorder [1]. Because of the varied nature of presenting signs and symptoms, kaposiform lymphangiomatosis is often misdiagnosed or diagnosed late. The imaging and presenting features of kaposiform lymphangiomatosis overlap with those

of central conducting lymphatic anomaly and generalized lymphatic anomaly. Central conducting lymphatic anomaly is another rare and complex lymphatic disorder characterized by enlargement of lymphatic channels (lymphangiectasia) and dysmotility, and distal obstruction can result in inadequate clearing of lymph, with resultant stasis and reflux. Generalized lymphatic anomaly is multisystem lymphatic disorder that involves multiple organs. Comparable to central conducting lymphatic anomaly and generalized lymphatic anomaly, intrathoracic and extrathoracic disease has been described in kaposiform lymphangiomatosis, including pleural and pericardial effusions, cystic lesions of the spleen and bony lesions [1].

The few case reports and small series [1–4] on kaposiform lymphangiomatosis have mainly emphasized the clinical and histopathological findings, with limited description of imaging findings. Here we present the imaging features of kaposiform lymphangiomatosis involving multiple organs and contiguous anatomical regions, highlighting the imaging features that are most suggestive of this diagnosis.

Materials and methods

This observational study was approved by our Committee on Clinical Investigation. We retrospectively reviewed the Vascular Anomalies Center and Department of Pathology databases for cases from 1995 to 2015 to identify patients with a histopathological diagnosis of kaposiform lymphangiomatosis (including the former term kaposiform lymphangioendothelioma). We reviewed patient demographics, clinical presentation and imaging studies of 25 patients and excluded 5 patients with no imaging study. Of the remaining 20 patients, 19 had more than one serial imaging study, with median follow-up of 17 months (range 1–75 months). Part of the cohort was included in a paper by Croteau et al. [1]; however two patients included by Croteau et al. were excluded because of unavailability of images and two additional patients who were not in the study by Croteau et al. were included. We performed statistical analysis using IBM SPSS for Windows version 21.0 (IBM Corp., Armonk, NY). We compared frequency distributions using the paired *t*-test. A P-value $\leq .05$ was considered statistically significant.

Results

The median age at onset of signs and symptoms was 6.5 years (range 3 months to 27 years); however the average age at diagnosis of a lymphatic anomaly was 8.4 years (range 8 months to 28 years). Eleven patients were male. The clinical characteristics of the cohort of patients are summarized in Table 1.

Clinical findings

Presenting features included respiratory symptoms 11/20 (55.0%), swelling/mass 5/20 (25%), bleeding 2/20 (10%), fracture 1/20 (5%) and no symptoms 1/20 (5%; incidentally found). The most common respiratory complaints were dyspnea ($n=6$), cough ($n=5$) and chest pain ($n=2$).

Three patients presented with unilateral lower extremity and buttock swelling, one with a discrete mass over the left posterior neck and another with a groin mass. Two patients presenting with other symptoms were also noted to have a swelling/mass on examination; a lesion involving the right scapula and chest wall in one, and breast and axilla in the other.

Bleeding was a presenting feature in two patients; however a total of eight patients had episodes of bleeding during the course of their disease, including five with one or more hemorrhagic effusions. Platelet counts were available in 15/20 patients. A total of 10/15 were found to have thrombocytopenia (thrombocytopenia is not a feature of generalized lymphatic anomaly or central conducting lymphatic anomaly) with a median platelet count of 58,000 (range 8,000–72,000; normal is 150,000–400,000). These included seven patients with bleeding and three without bleeding. Only 5/10 (50%) patients with thrombocytopenia had associated splenomegaly, so cause of thrombocytopenia is not clear.

Imaging findings

Imaging was performed using multiple modalities at the discretion of the treating physician: CT ($n=17$), MRI ($n=13$), US ($n=8$) and plain radiographs ($n=17$). The imaging modalities employed in each patient reflected the changing imaging trends over the course of the 20-year study period (i.e. MRI would now often be favored over CT in such cases). Moreover, there was extreme variability of specific sequence parameters because of continued modifications in MRI techniques over such a long time period as well as the multiple institutions supplying the original scans. Fat-suppressed pre-contrast fluid-weighted sequences and post-contrast T1-weighted images were obtained in all patients with MRI scans. Fat saturation of pre-contrast T1 was not routinely performed.

Serial imaging was available in 19 of the 20 patients. The thoracic cavity was the most common region involved (20/20) followed by abdomen/pelvis (13/20), bone (12/20), and muscle (9/20). Affected sites included mediastinum 20/20 (100%), lung parenchyma 18/20 (90%), pleural cavity 17/20 (85%), retroperitoneum 13/20 (65%), bone 12/20 (60%), pericardial cavity 10/20 (50%), abdominal viscera 10/20(50%), mesentery 9/20 (45%) and muscles 9/20 (45%).

Table 1 Clinical characteristics and disease distribution

Patient#	Gender	Age at presentation (years)	Age at diagnosis (years)	Presenting symptoms	Thoracic Mediastinum (M) Parenchymal (Pa) Pleural (Pl)	Abdominal Retroperitoneal (RP) Visceral (V) Ascities (A)	MSK Bone (B) Muscle (M)
1	Male	5.2	5.3	Dyspnea	M, Pa, Pl		
2	Male	1.5	1.5	Epistaxis, bruising	M, Pa, Pl	V	B, M
3	Female	2.0	2.7	Right thigh swelling	M, Pa, Pl	RP, V	B, M
4	Female	9.0	12.0	Left thigh swelling	M, Pa, Pl	RP, V	B, M
5	Male	3.2	7.2	Dyspnea	M, Pa, Pl	V	
6	Female	16	17.5	Chest pain	M, Pa, Pl	RP	
7	Male	4.0	8.5	Dyspnea	M, Pa, Pl	RP	
8	Female	10	10.8	Dyspnea, orthopnea	M, Pa, Pl	RP	B, M
9	Male	13.2	19.7	Cough	M, Pa, Pl	RP	
10	Male	7.0	16.2	Right femur fracture	M, Pa, Pl	V	B, M
11	Male	1.7	2.2	Epidural hematoma, scleral hemorrhage	M, Pa, Pl	RP, V	B
12	Male	4.0	5.1	Dyspnea, cough, lethargy	M, Pa, Pl	RP	
13	Female	6.0	8.6	Left posterior neck swelling/mass	M, Pa	RP, V,	B, M
14	Male	0.4	0.7	Incidental	M, Pa, Pl	RP, V	
15	Male	1.5	1.6	Cough, fever	M, Pa, Pl	RP, V	B
16	Female	10.0	30.0	Left leg and buttock swelling	M, Pl	RP, V, A	B, M
17	Female	13.1	14.9	Cough, chest pain	M, Pa	RP	
18	Female	12.3	12.4	Cough	M, Pa, Pl	RP, A	B
19	Male	19	19.8	Scrotal swelling		RP, A	B, M
20	Female	27	28	Dyspnea	M, Pa, Pl	RP, V, A	B, M

MSK musculoskeletal

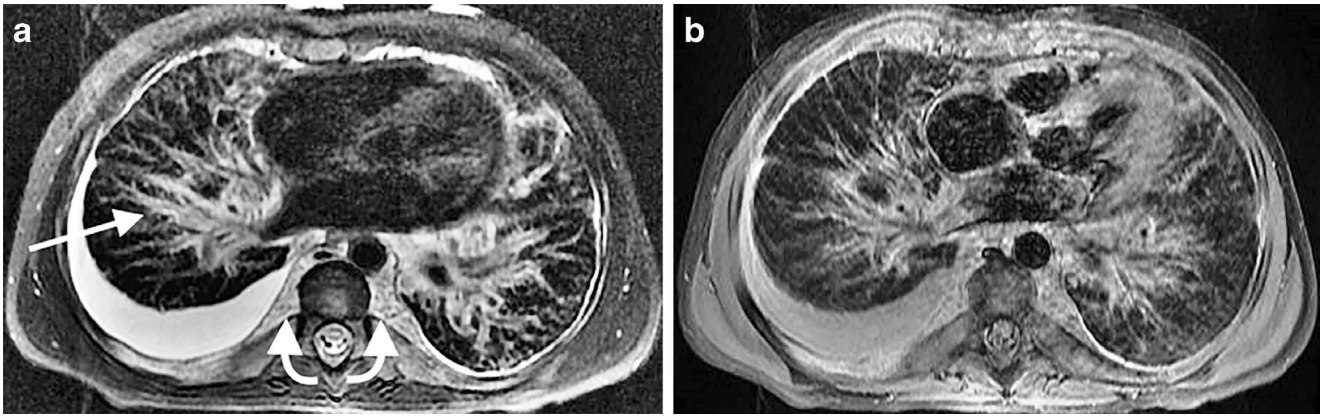

Fig. 1 Chest MRI in 10-year-old girl with kaposiform lymphangiomatosis. **a** Axial T2-W fat-saturated sequence shows high signal abnormality in the mediastinum that extends along the bronchovascular bundles (*straight arrow*). There is a right pleural effusion and bilateral retrocrural soft-tissue thickening (*curved arrows*). **b** Axial T1-W fat-saturated post-contrast image shows enhancement of the infiltrative soft tissue along the bronchovascular bundles and in the retrocrural regions

Chest

All (100%) of the patients had posterior mediastinal and hilar disease. Involvement of the anterior mediastinum was seen in 14/20 (70%). The characteristic pattern of kaposiform lymphangiomatosis was infiltrative soft-tissue thickening (20/20) or mass of low attenuation on CT. This was heterogeneously hyperintense on fluid-weighted MRI sequences, with moderate to intense post-contrast enhancement seen in all patients (Fig. 1). Infiltrative enhancing soft-tissue thickening followed the lymphatic distribution along bronchovascular bundles. In the anterior mediastinum, the soft-tissue thickening around the blood vessels and airways mimicked the shape of a mass (10/14).

Lung parenchymal involvement was seen in 18/20 (90%) patients and was characterized by extension of soft tissue along the bronchovascular bundles. However there was significant variability in the extent and distribution of the parenchymal findings, ranging from segmental to diffuse perivascular interlobular septal thickening, with variable extension to the sub-pleural region (Fig. 2). Ground-glass or alveolar opacities were seen in children with clinical evidence of superimposed infection. Pulmonary parenchymal involvement was asymmetrical in 50% of the patients, without left or right predilection.

A total of 17/20 (85%) patients had pleural effusions (bilateral in 9). The effusions were either serosanguinous, chylous (high lymphocyte count, milky white fluid with high triglyceride level) or chyle mixed with blood. On sonography, the effusions appeared largely anechoic, with some low-level internal echoes. In all of the patients who had a CT scan, the effusions were of low attenuation (slightly denser than water). The effusions were hyperintense on fluid-weighted MRI sequences.

A total of 16/20 patients had follow-up imaging of the chest. The follow-up imaging was performed because of worsening symptoms or to assess response to treatment. The parenchymal disease worsened in 11 (increased extent of bronchovascular or septal thickening or worsening alveolar opacities), was stable in 3 and improved in 2. Mediastinal disease increased in extent in 10 patients, remained stable in 5 and improved in 1. Pleural disease progression was difficult to accurately assess because there were multiple interventions, including drainage and pleurodesis. The patients with radiologic evidence of improved

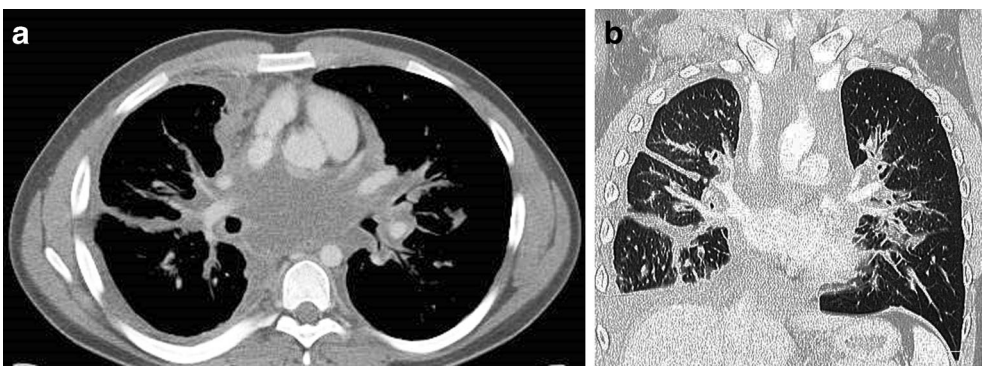

Fig. 2 Chest involvement in a 13-year-old boy with kaposiform lymphangiomatosis. **a** Axial contrast-enhanced CT shows infiltrative low-density soft tissue in the mediastinum and extending along the bronchovascular bundles. **b** Coronal CT reformat on lung windows shows parenchymal bands, interlobular septal thickening and ground-glass opacity in the right lung

Table 2 Distribution of visceral involvement

Viscus	Findings	Number of patients (*n*)	Associated finding
Spleen	Splenomegaly with cystic lesions	6	4 patients had associated hepatomegaly
	Splenomegaly without lesions	1	
Kidney	Bilateral renal cysts with unilateral nephromegaly	2	
Pancreas	Cystic lesions	2	

parenchymal or mediastinal disease underwent multiple surgical and interventional procedures and received medical therapy.

Abdomen

Visceral abnormalities were seen in 11/20 (55%) patients at initial imaging. In all of these patients, clusters of round cystic lesions were identified in the abdominal viscera with or without organomegaly (Table 2). On MRI, the round lesions were heterogeneous and hyperintense on fluid-weighted sequences, hypodense (but denser than water) on CT and anechoic to hypoechoic on ultrasonography (Fig. 3). Follow-up imaging was available in 9/10 patients with visceral lesions; splenectomy was performed in 2 patients. In the remainder, the number of lesions increased in two, remained stable in four and decreased in one (treated with sirolimus), with no significant difference in imaging characteristics.

Retroperitoneal disease 16/20 (80%), characterized by enhancing infiltrative soft tissue, almost always involved the retrocrural region (Fig. 4), with extension to the mesentery (9/16) along the mesenteric vessels, the hepatic hilum (6/16) along the portal vein, and one or both renal hila (5/16) along their vessels. Follow-up imaging, available in 15/16 patients, showed stable (8/15) or increased extent of signal abnormality (7/15).

Ascites was present in 4/20 patients at presentation; however during the course of disease ascites developed in 5 more patients (9/20). Other, infrequent involvement included rectosigmoid wall thickening with cystic lesions (1/20), and urinary bladder and adjacent bowel wall thickening with infiltrating soft tissue in the perineum and with cystic lesions (1/20).

Musculoskeletal

Bony lesions were present in 12/20 (60%) patients. Seven patients demonstrated progression, with an increase in the number of bones involved or the extent of osseous disease. Bony lesions were lytic (punched out), typically with cortical sparing (Fig. 5). One patient had multiple fractures of the femur and humerus over time. The osseous changes were readily visualized with plain radiography or CT, but bone marrow changes and enhancing infiltrative soft tissue were best seen by MRI. The osseous abnormality was characterized by increased signal on fluid-weighted sequences, with heterogeneous enhancement seen on administration of contrast

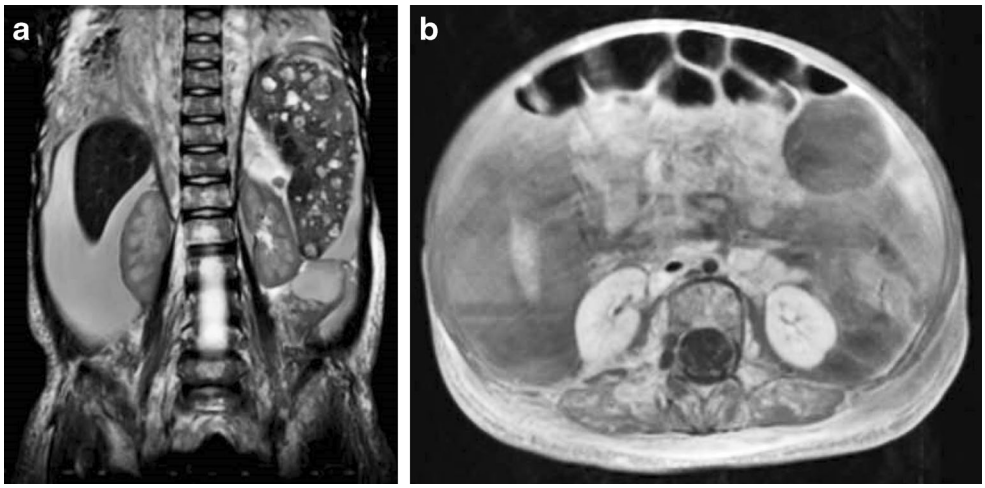

Fig. 3 Visceral abnormalities on MRI in a 2-year-old girl with kaposiform lymphangiomatosis. **a** Coronal short tau inversion recovery sequence shows multiple cystic lesions throughout the spleen, with associated splenomegaly. Note the large amount of ascites. Lesions are in multiple thoracic, lumbar and upper sacral vertebral bodies and bilateral iliac bones. Adjacent paraspinal soft-tissue and retrocrural involvement are also noted. **b** Axial post-contrast MR image shows abnormal enhancement of the vertebral body and surrounding muscles, and subcutaneous disease

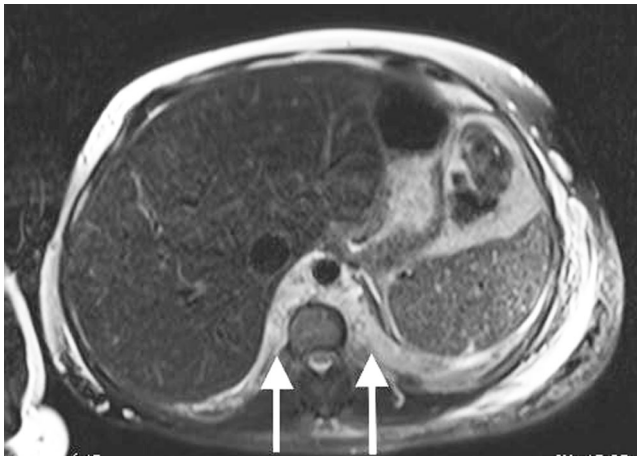

Fig. 4 Retroperitoneal involvement on MRI in a 24-year-old woman with kaposiform lymphangiomatosis. Axial T2-W fat-saturated image shows hyperintense high-signal infiltrative tissue in the retroperitoneum (*arrows*), left abdominal wall musculature and subcutaneous fat

agent. Poorly defined, high-signal soft tissue adjacent to bony lesions was seen in 10 patients.

The bony lesions were asymmetric in distribution. Involvement of the axial skeleton (vertebral column, rib cage, sternum and cranium) was seen in 8/12 patients, whereas the appendicular skeleton (shoulder girdle, pelvic girdle, upper and lower extremities) was involved in 6/12. The vertebral bodies were the most common sites of bony involvement 8/12 (67%) (Fig. 3). Frequently, multiple contiguous (spine) and noncontiguous bones were involved, including femur, humerus, ribs and pelvis. Table 3 demonstrates distribution of bony involvement.

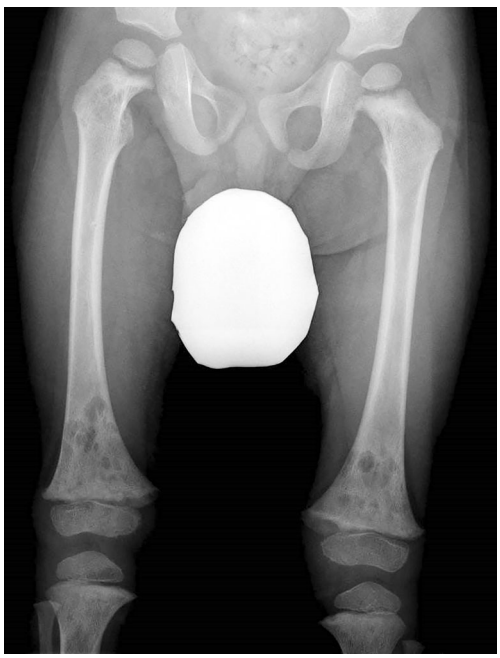

Fig. 5 Bony involvement on anteroposterior radiograph in an 18-month-old boy with kaposiform lymphangiomatosis. Multiple lytic lesions are seen in the distal femur and proximal tibia bilaterally, with preservation of the cortex

MR imaging was available in only 13/20 patients, so not all 20 patients were evaluated for muscle involvement. The muscles were involved in 9 patients at presentation and appeared as an infiltrative abnormality on fluid-weighted MR sequences. Stranding of the adjacent subcutaneous fat with sparing of skin was present in 11 patients, including 6 who also had an adjacent osseous abnormality. Multiple groups of muscles were involved in more than one patient. The muscle groups involved were paravertebral ($n=4$), lower posterior spinal ($n=3$), lateral and posterior chest wall ($n=2$), gluteal ($n=2$), all compartments of the thigh ($n=2$), anterior and lateral abdominopelvic wall ($n=3$) and all compartments of the upper arm ($n=1$). No macrocystic lymphatic malformation was identified.

Lymphatic channel imaging

Eight patients had a dedicated study of lymphatic function, including six with dynamic intranodal lymphangiography and two with lymphoscintigraphy. Intranodal lymphangiography showed abnormal contour of the terminal portion of thoracic duct and emptying into the venous angle (1/6), and increased number of dilated inguinal channels and reflux into abnormal lymphatics in one or more distributions in all patients (Fig. 6). Reflux of contrast agent was seen into the following channels: femoral/iliac (3/6), jugular/cervical (5/6), phrenic/pleural/thoracic (5/6), mediastinal/pericardial (5/6), lumbar/mesenteric (6/6) and retroperitoneal (1/6). In

Table 3 Distribution of bony involvement

Location	Bones	Number of patients (*n*)
Axial skeleton	Skull base	1
	Cervical spine	3
	Sternoclavicular joint	1
	Thoracic spine	6
	Lumbar spine	3
	Sacrum	4
Appendicular skeleton	Scapula	2
	Humerus	3
	Radius	1
	Ulna	1
	Ilium	4
	Pelvic bone	4
	Ischium	4
	Femur	4
	Tibia	1

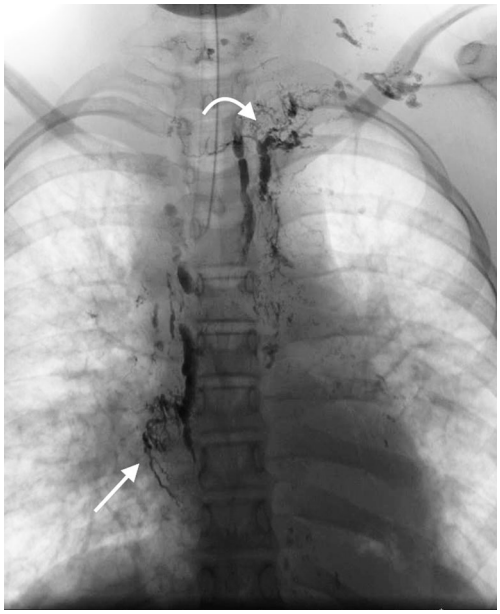

Fig. 6 Intranodal lymphangiogram in a 12-year-old girl with kaposiform lymphangiomatosis. There is reflux of contrast agent into the mediastinal lymphatics (*straight arrow*). Multiple collaterals are seen in the left supraclavicular region associated with non-visualization of the terminal portion of the thoracic duct, which is replaced by multiple small collaterals at the venous angle and a prominent parallel mediastinobronchial lymphatic channel to the left of thoracic duct (*curved arrow*)

one patient there was no progression of contrast agent into the thorax. Lymphoscintigraphy showed delayed transit time in the lymphatic channels (2/2), with dermal back flow in one of the two patients.

Histopathology

Pathological material was available in all 20 patients with kaposiform lymphangiomatosis. The pathological findings were based upon surgical biopsies of mediastinal soft tissues ($n=7$), lung ($n=4$), thymus ($n=3$), pericardium ($n=3$), skin ($n=5$), pleura ($n=2$), bone ($n=2$), spleen ($n=2$), subcutaneous tissue ($n=1$) and gastrointestinal mucosa ($n=1$) as well as autopsies ($n=3$). Immunohistochemical stains were also available in one or more tissue samples from 15 of the 20 patients: D2-40 ($n=15$), CD31 ($n=9$), CD34 ($n=7$), factor VIII ($n=6$), LYVE-1($n=5$), smooth muscle actin ($n=9$), PROX-1 ($n=1$) and GLUT-1 ($n=2$). The affected tissues showed abnormal, dilated lymphatic channels, generally with minimal or no muscularization (Fig. 7). These were accompanied by dispersed small clusters of spindle cells without distinct lumens and with erythrodiapedesis. The spindle cells did not have nuclear atypia and often contained abundant

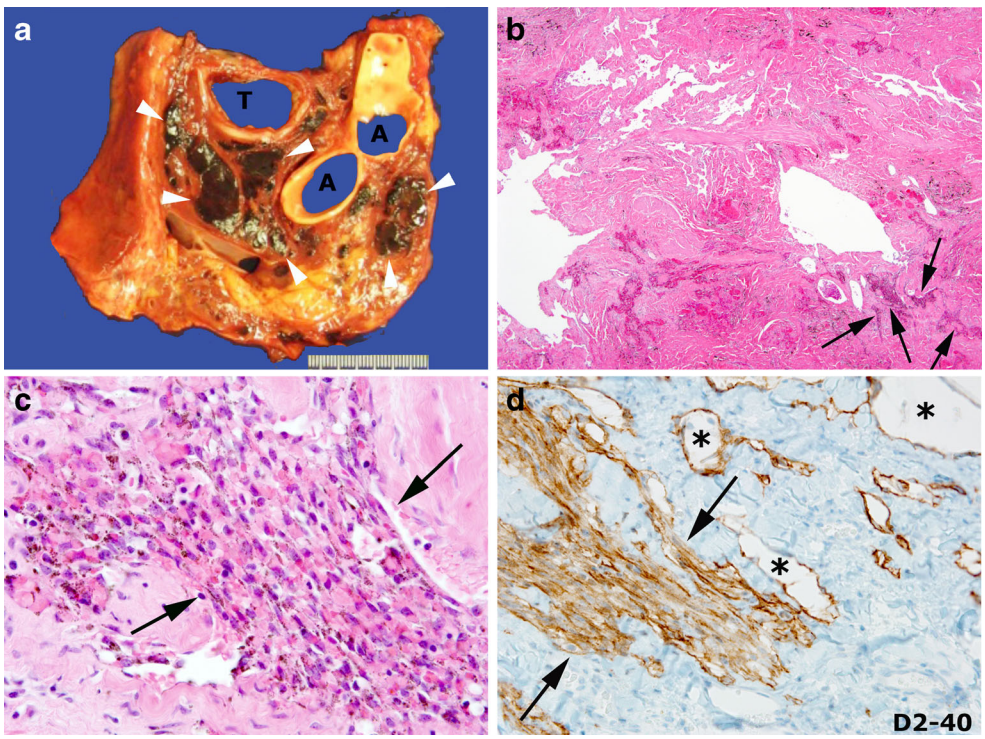

Fig. 7 Pathological findings. **a** Transverse section through the mediastinal autopsy block shows spongy connective tissue with dilated lymphatic channels containing thrombus (*arrowheads*). **b** Pathology shows abnormal and dilated lymphatic channels, some filled with blood, within dense connective stroma. Small irregular cellular clusters are indicated by arrows (hematoxylin & eosin [H&E] × 40 magnification). **c** A cluster composed of kaposiform, spindle-shape, hemosiderotic lymphatic endothelial cells (*arrows*) is accompanied by erythrodiapedesis (H&E × 400 magnification). **d** D2-40, an immunohistochemical lymphatic endothelial marker, highlights spindle cells (*arrows*) and adjacent abnormal lymphatic vessels (*asterisks*) (D2-40 immunostain × 100 magnification). *A* aorta, *T* trachea

cytoplasmic hemosiderin. Their immunopositivity for D2-40, PROX-1, LYVE-1, CD31, and factor VIII, in all instances accompanied by immunonegativity or focal and weak immunopositivity for CD34, was consistent with a lymphatic endothelial phenotype. In occasional cases, some foci of spindle cells were larger and sometimes confluent and similar to kaposiform hemangioendothelioma. Frank local hemorrhages as well as blood-filled lymphatic channels were sometimes observed. The spleen, in addition to having lymphatic cysts, also showed focal or diffuse expansion of the cords of Billroth and dilated sinuses lined by spindled and hemosiderotic lymphatic endothelium.

Discussion

Lymphatic malformations likely arise from anomalous embryogenesis of the lymphatic system. Simple lymphatic malformations are usually readily diagnosed by clinical examination and imaging. In contrast, complex lymphatic anomalies often require analysis of clinical, imaging, hematological and histological features, and even with all these data, the diagnosis might not be readily apparent [5, 6]. Kaposiform lymphangiomatosis is a type of complex lymphatic anomaly that exhibits features of both malformation and neoplasia. The onset of symptoms in childhood is suggestive of aggressive disease [7]. The histopathology combines malformed lymphatic channels and a proliferative spindle cell component. The spindle cell component in kaposiform lymphangiomatosis is usually sparse, with dispersed and poorly marginated clusters of parallel-oriented spindle cells, whereas in kaposiform hemangioendothelioma the growth is primarily solid with more defined, rounded, confluent vascularized nodules with microthrombi [1].

More than 90% of our patients were referred to our vascular anomalies center at a later stage of their disease (median time from initial symptoms to diagnosis was 11.5 months), often with a diagnosis of lymphangiomatosis. Several factors contributed to this interval, including nonspecific signs and symptoms such as shortness of breath, lymphedema, thrombocytopenia with or without splenomegaly, and limited access to medical care. Lack of detailed description of imaging findings of kaposiform lymphangiomatosis in the literature might have contributed to delayed consideration of this diagnosis.

Kaposiform lymphangiomatosis shares overlapping patterns of clinical symptoms, anatomical location, imaging features and complications with other lymphatic anomalies such as central conducting lymphatic anomaly and generalized lymphatic anomaly. Microscopically, central conducting lymphatic anomaly and generalized lymphatic anomaly are characterized by variable-size thin-walled lymphatic channels lined by flattened, D2-40-immunopositive endothelial cells and lumens that are empty or contain protein or blood [8, 9].

In central conducting lymphatic anomaly, there is enlargement of lymphatic channels (lymphangiectasia), either from impaired physiology (motility) or distal functional/mechanical obstruction causing inadequate clearing of lymph, with resultant stasis and reflux. Manifestations such as chylothorax, pulmonary lymphangiectasia, chylous ascites, intestinal lymphangiectasia, protein-losing enteropathy, cutaneous vesicles and superficial chylous leaks reflect the sites of involvement [8]. The anatomical and imaging spectrum of kaposiform lymphangiomatosis is very similar to that of central conducting lymphatic anomaly. On lymphangiography it is difficult to differentiate kaposiform lymphangiomatosis from central conducting lymphatic anomaly, as evident from the findings in our patients. Lytic osseous lesions resulting from dilated intraosseous channels sparing the cortex, with or without associated soft-tissue involvement, are also common in both entities. Likewise, mediastinal disease extending to the hila is nearly universal in both. Infiltrative soft-tissue thickening along the bronchovascular bundle and interlobular septal thickening are also common findings in both. However, moderate enhancement of the infiltrative soft-tissue thickening on MRI/CT, aggressive clinical course and thrombocytopenia favor kaposiform lymphangiomatosis over central conducting lymphatic anomaly; in this setting the characteristic histopathology in tissue samples from involved sites is confirmatory.

The osseous findings in kaposiform lymphangiomatosis, with multiple non-contiguous lytic lesions sparing the cortex, also overlap with those of generalized lymphatic anomaly. The preservation of the cortex differentiates these conditions from Gorham-Stout disease [8]. However, unlike generalized lymphatic anomaly, where the ribs are the most common site of involvement [10], in kaposiform lymphangiomatosis the thoracic spine is the most common site, although distribution of lesions is not a significant differentiator between the conditions. Like generalized lymphatic anomaly, the number of bones involved and the size of the lesions increase over time. Splenomegaly with cysts was also seen, similar to generalized lymphatic anomaly. However, unlike generalized lymphatic anomaly, most patients with kaposiform lymphangiomatosis (75%) had infiltrative soft-tissue lesions adjacent to osseous changes. In kaposiform lymphangiomatosis, pleural effusions and ascites were more dense on CT than in generalized lymphatic anomaly, likely because of the increased attenuation of blood mixed with chyle. Thoracic involvement is also much more extensive in kaposiform lymphangiomatosis. Mediastinal disease extending to the hila, enhancing infiltrative soft-tissue thickening along the bronchovascular bundles and interlobular septal thickening are uncommon in generalized lymphatic anomaly [10]. In addition, retroperitoneal enhancing infiltrative soft-tissue thickening, hemorrhagic effusions, a deteriorating clinical course, or associated moderate thrombocytopenia (50–100,000/μl) should raise the suspicion

of kaposiform lymphangiomatosis. Thrombocytopenia is not a characteristic feature of generalized lymphatic anomaly. Furthermore, kaposiform lymphangiomatosis appears to be less responsive to medical therapy than generalized lymphatic anomaly [11, 12].

The imaging features of muscle disease in kaposiform lymphangiomatosis were similar to those of kaposiform hemangioendothelioma, with involvement of multiple planes. Unlike kaposiform hemangioendothelioma, however, cutaneous involvement is rare in kaposiform lymphangiomatosis. Kaposiform lymphangiomatosis is almost always multifocal, whereas kaposiform hemangioendothelioma is most often unifocal. Kaposiform hemangioendothelioma typically presents in early infancy with a characteristic purpuric, cutaneous lesion [13–15], whereas kaposiform lymphangiomatosis presents later in childhood, typically with respiratory symptoms and uncommonly with cutaneous manifestations. In kaposiform hemangioendothelioma, thrombocytopenia is usually moderate-to-severe, while in kaposiform lymphangiomatosis it is mild-to-moderate. The mechanism of thrombocytopenia in kaposiform hemangioendothelioma is likely related to platelet consumption within fibrin thrombi, while the mechanism in kaposiform lymphangiomatosis remains unclear [15, 16]. Kaposiform hemangioendothelioma also appears to respond more favorably to medical therapy in comparison to kaposiform lymphangiomatosis [10, 17].

Conclusion

Kaposiform lymphangiomatosis has overlapping imaging features with central conducting lymphatic anomaly and generalized lymphatic anomaly. Presence of enhancing infiltrative soft tissue in the mediastinum and retroperitoneum, hemorrhagic effusions and moderate thrombocytopenia (50–100,000/μl) should favor the diagnosis of kaposiform lymphangiomatosis.

Acknowledgments We are very grateful to David Zurakowski, PhD, MA, MS, Statistics, Director of Biostatistics at Boston Children's Hospital, for his help in biostatistics.

Compliance with ethical standards

Conflicts of interest None

References

1. Croteau SE, Kozakewich HP, Perez-Atayde AR et al (2014) Kaposiform lymphangiomatosis: a distinct aggressive lymphatic anomaly. J Pediatr 164:383–388
2. Safi F, Gupta A, Adams D et al (2014) Kaposiform lymphangiomatosis, a newly characterized vascular anomaly presenting with hemoptysis in an adult woman. Ann Am Thorac Soc 11:92–95
3. Detaille T, Joomye R, Barrea C et al (2010) Acute life-threatening presentation of unknown lymphatic malformation. Am J Emerg Med 28:1062.e1061–1063
4. Debelenko L, Marler J, Perez-Atayde A et al (2004) Kaposiform lymphangiomatosis: an aggressive variant of lymphangiomatosis (LA). In: Laboratory investigation, vol. 84. Nature Publishing Group, New York, p 269
5. Trenor CC 3rd, Chaudry G (2014) Complex lymphatic anomalies. Semin Pediatr Surg 23:186–190
6. Fernandes VM, Fargo JH, Saini S et al (2015) Kaposiform lymphangiomatosis: unifying features of a heterogeneous disorder. Pediatr Blood Cancer 62:901–904
7. Enjolras O, Mulliken JB, Kozakewich HP (2013) Vascular tumors and tumors like lesions. In: Mulliken JB, Burrows PE, Fishman SJ (eds) Mulliken and Young's vascular anomalies: hemangiomas and malformations, 2nd edn. Oxford University Press, New York, pp 259–326
8. Fishman SJ (2013) Slow-flow vascular malformations. In: Mulliken JB, Burrows PE, Fishman SJ (eds) Mulliken & Young's vascular anomalies: hemangiomas and malformations. Oxford University Press, New York
9. Tazelaar HD, Kerr D, Yousem SA et al (1993) Diffuse pulmonary lymphangiomatosis. Hum Pathol 24:1313–1322
10. Lala S, Mulliken JB, Alomari AI et al (2013) Gorham-Stout disease and generalized lymphatic anomaly — clinical, radiologic, and histologic differentiation. Skeletal Radiol 42:917–924
11. Hammill AM, Wentzel M, Gupta A et al (2011) Sirolimus for the treatment of complicated vascular anomalies in children. Pediatr Blood Cancer 57:1018–1024
12. Reinglas J, Ramphal R, Bromwich M (2011) The successful management of diffuse lymphangiomatosis using sirolimus: a case report. Laryngoscope 121:1851–1854
13. Lyons LL, North PE, Mac-Moune Lai F et al (2004) Kaposiform hemangioendothelioma: a study of 33 cases emphasizing its pathologic, immunophenotypic, and biologic uniqueness from juvenile hemangioma. Am J Surg Pathol 28:559–568
14. Zukerberg LR, Nickoloff BJ, Weiss SW (1993) Kaposiform hemangioendothelioma of infancy and childhood. An aggressive neoplasm associated with Kasabach-Merritt syndrome and lymphangiomatosis. Am J Surg Pathol 17:321–328
15. Croteau SE, Liang MG, Kozakewich HP et al (2013) Kaposiform hemangioendothelioma: atypical features and risks of Kasabach-Merritt phenomenon in 107 referrals. J Pediatr 162:142–147
16. Enjolras O, Mulliken JB, Wassef M et al (2000) Residual lesions after Kasabach-Merritt phenomenon in 41 patients. J Am Acad Dermatol 42:225–235
17. Haisley-Royster C, Enjolras O, Frieden IJ et al (2002) Kasabach-Merritt phenomenon: a retrospective study of treatment with vincristine. J Pediatr Hematol Oncol 24:459–462